Pergamon

Cement and Concrete Research, Vol. 25, No. 6, pp. 1237-1245, 1995
Copyright © 1995 Elsevier Science Ltd
Printed in the USA. All rights reserved
0008-8846/95 $9.50+.00

0008-8846(95)00116-6

EFFECTS OF THE TEMPERATURE AND RELATIVE HUMIDITY ON THE STRUCTURE OF C–S–H GEL

Xiandong Cong and R. James Kirkpatrick
ACBM Center and Department of Geology
University of Illinois, Urbana, IL., 61801, U. S. A.

(Refereed)
(Received October 25, 1994; in final form April 17, 1995)

ABSTRACT

This paper describes the structural changes of C–S–H caused by curing at different relative humidities (R. H.) and temperatures using XRD, ^{29}Si NMR and thermal analysis. The results show that within the relative humidity range studied (9%–100%), the polymerization of C–S–H does not change, but that the local structure becomes more disordered with decreasing R. H. Heating of C–S–H results in increasing polymerization and structural disorder, and decreasing basal–spacing. It appears that decreasing relative humidity removes interlayer water molecules but that heating removes both water molecules and OH^- groups. Thermal behaviors of jennite and 1.4–nm tobermorite are also studied and compared with those of C–S–H.

Introduction

One of the important characteristics of calcium silicate hydrate gel (C–S–H) is its structural and compositional diversity, of which structural variation at different curing conditions is an important example. Previous work has shown that C–S–H samples formed at elevated temperatures are more polymerized than those formed at room temperature under otherwise similar conditions [1, 2, 3], and that C–S–H samples cured at low relative humidities (R. H.) have smaller d–spacings than those cured at high R. H [4, 5].

In this paper, we examine the structural changes in synthetic C–S–H with C/S ratio from 1.13 and 1.56 cured at relative humidities from 9% to 100% and temperatures from 25 to 200°C, using ^{29}Si NMR spectroscopy, XRD and thermal analysis, and discuss the importance of these changes to the overall structure of C–S–H. we also study the thermal behaviors of 1.4–nm tobermorite and jennite and compare the results with those for C–S–H.

Experimental

The C–S–H samples used in this study were selected from the three C–S–H series described previously by Cong and Kirkpatrick [6]. Briefly, samples of SCFUM series were prepared by aqueous reaction of CaO and fumed silica. Samples of SEWCS series were prepared by hydration of highly reactive β–C_2S. All samples used here are single phase C–S–H as shown by XRD and NMR. The C/S molar ratios were determined by X–ray fluorescence analysis of bulk samples. Samples for the relative humidity study (SCFUMf, C/S=1.13 and SEWCS4, C/S=1.48) were first separated from the solution via filtering and divided into three parts. Each part was stored in a desiccator with the desired relative humidity and cured at room temperature for 5 weeks. The relative humidities were controlled by the following saturated salt solutions [1]: H_3PO_4 (*ca.* 9% R. H.), $Ca(NO_3)_2{\cdot}4H_2O$ (*ca.* 51% R. H.) and KNO_3 (*ca.* 71% R. H.). Although no attempt was made to control the R. H. during the NMR data acquisition, the R. H. of the samples was expected to remain unchanged because the samples were loaded quickly and rotors were sealed tightly. A slurry (water saturated) of each sample was also examined with ^{29}Si NMR by directly loading the unfiltered original reaction product into an O–ring sealed 7 mm NMR rotor. All operations were inside a glove bag filled with N_2 gas to prevent carbonation.

The effects of heating were examined for three air–dried phase–pure C–S–H samples (SCFUMe with C/S = 1.19, SEWCS3 with C/S = 1.56 and CSHFS2 with C/S = 1.50). The samples were heated at 110°C for 2 hours and 200°C for 3 hours in a vacuum oven and then examined by ^{29}Si NMR and XRD.

^{29}Si MAS NMR and ^{1}H–^{29}Si CPMAS NMR spectra were collected under the conditions described elsewhere [6, 7]. TG and DSC data for some air–dried C–S–H samples were collected between 20 and 670°C using a Netzsch STA 409/414–2 Simultaneous Thermal Analyzer with a heating rate of 5°C/min and air flow rate of 75cc/min.

Results

Effect of Relative Humidity

The ^{29}Si MAS NMR spectra of the two C–S–H samples cured at different relative humidities contain both Q^1 and Q^2 peaks at *ca.* -79 and *ca.* -85 respectively (FIG. 1), and the relative intensities of the two peaks do not change systematically with the relative humidity (TABLE 1). However, the full widths at half height (FWHH) of both the Q^1 and Q^2 peaks increase with decreasing R. H., indicating increased local structure disorder. The FWHH's of the 9% R. H. samples are comparable to those of air–dried samples discussed before [6]. The spectra of the slurry samples are similar to those cured at 71% R. H., but the relative intensity of the Q^2 peak appears to be less than those in other spectra, possibly indicating that the polymerization is lower when the samples are in direct contact with solution. The signal/noise ratio for the slurry samples is low due to the small sample size, however, and this conclusion is uncertain.

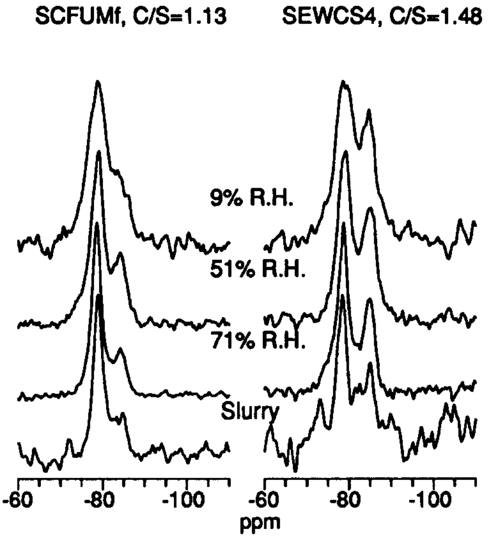

FIG. 1

^{29}Si MAS NMR spectra of selected C–S–H cured at different relative humidities as marked in the figure.

---

[1] CRC Handbook of Chemistry and Physics, 67th edition, ppE–42.

TABLE 1

Relative Intensity (I%) and FWHH (ppm) of ^{29}Si NMR Spectra for C–S–H Samples Cured at Different Relative Humidities (R. H.). FWHH Values in Parentheses Are Measured from the CPMAS Spectra.

Sample	R. H. (%)	Q^1		Q^2	
		I%	FWHH	I%	FWHH
SEWCS4 C/S=1.48	Slurry	unavailable due to low S/N			
	71	64	3.3(3.1)	36	3.7(3.5)
	51	57	3.7(3.2)	43	4.4(4.1)
	9	65	5.5(4.2)	35	4.2(4.5)
SCFUMf C/S=1.13	Slurry	71	2.9	29	4.2
	71	72	3.0	28	4.2
	51	70	3.2	30	4.2
	9	73	4.6	27	5.0

The ^{1}H–^{29}Si CPMAS NMR spectra of the cured samples are similar to the corresponding MAS spectra, and both Q^1 and Q^2 cross polarize well (FIG. 2). The relative intensities of both Q^1 and Q^2 peaks vary as a function of contact time and these variations can be described by Eq. 6 of reference [7] (FIG. 3). However, it is clear that at 51% and 71% R. H. the contact time dependence of the relative intensities is not single exponentials and indicates the presence of multiple components of proton spin system. This is expected because at higher R. H. more water molecules are present and contribute to the proton relaxation process. At 9% R. H., however, the contact time dependence appears to be single exponential, probably due to reduced water content, and the observed data can be well fit with the Equation mentioned above (FIG. 3). For Q^1 sites, T_{CP}= 0.47 milliseconds (ms) and $T_{1\rho}^H$= 7.88 ms. For Q^2 sites, T_{CP}= 0.63 ms and $T_{1\rho}^H$= 17.79 ms. These results are in good agreement with the corresponding average values of air-dried C–S–H samples [7].

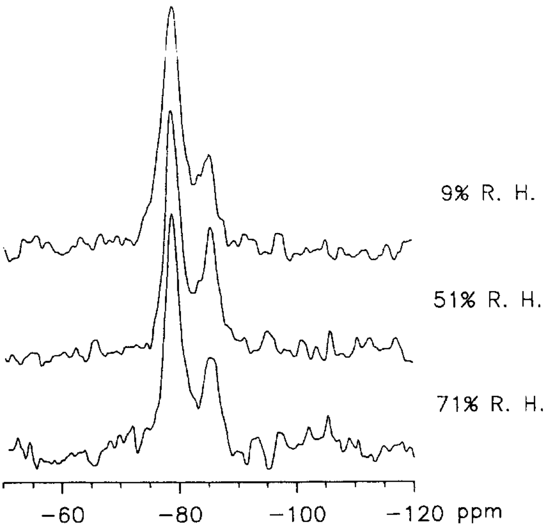

FIG. 2

^{1}H–^{29}Si CPMAS spectra of C–S–H SEWCS4 cured at different relative humidity as marked in the figure. The contact time used is 1 ms for all spectra.

The FWHH of the Q^1 peaks in the CPMAS spectra are non–systematically narrower than those of the corresponding MAS spectra (TABLE 1), but those of the Q^2 peaks appear no change. The FWHH decrease for samples cured at 9% R. H. is about 24%, but only 13 and 6% samples cured at 51 and 71% R. H. This progressive decrease of FWHH with decreasing R. H. is due to increased effectiveness of proton decoupling (^{1}H decoupling was turned on during data acquisition in the CP experiments). As relative humidity decreases, the amount of water in the C–S–H structure also decreases, resulting in decreased motion of water molecules and stronger ^{1}H–^{29}Si coupling. This interpretation is consistent with the variation of signal/noise ratio of the CPMAS spectra, which increases from about 15 at 71% R. H. to about 18 at 9% R. H. However, it is not clear why CP and proton decoupling has no obvious effects on FWHH of the Q^2 peak. One possible explanation is that, since Q^1 sites are mostly in dimers [7] and the structural regions with high dimer concentration may be more open than the regions with long silicate chains, thus contain more water molecules. As decreasing R. H. drives out the water molecules, the effects are more important to dimer-rich regions than to long-chain regions.

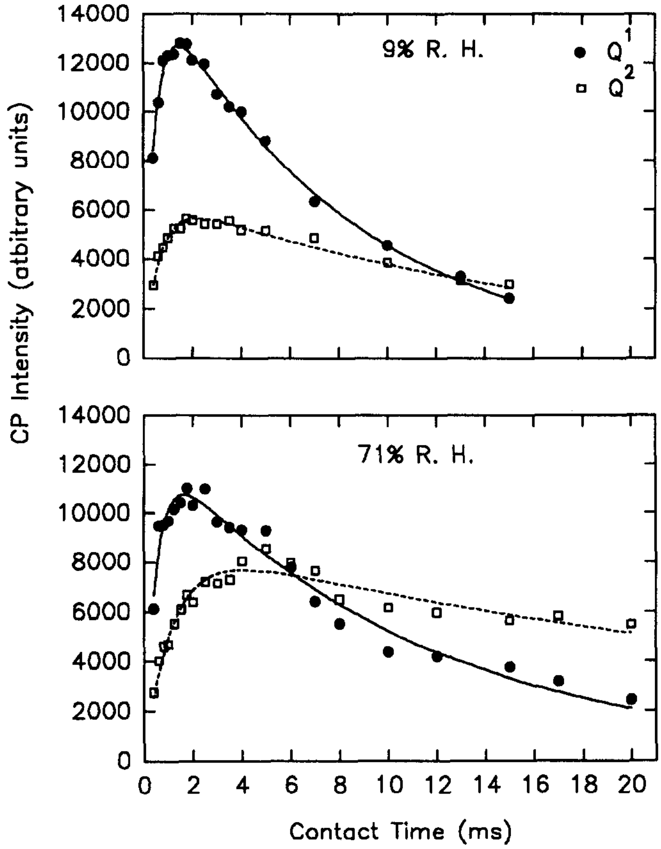

FIG. 3

Contact time dependence of the relative intensity of the CP spectra of C-S-H sample SEWCS4 cured at different R. H. The curve for the 9% R. H. cured sample shows a perfect exponential decay (top), but the curve for the 71% R. H. sample shows multiple components of proton spin system (bottom).

Heated Samples

The most obvious effect of heating the C-S-H samples on their XRD pattern is decrease of the basal spacing and the broadening of all the peaks (FIG. 4). These observations indicate that heating of C-S-H removes the interlayer water and increases the long range disorder. The average a and b pseudo unit cell dimensions do not change significantly, although the increased peak widths indicate a wider range at higher R. H.

The ^{29}Si MAS NMR spectra of heated C-S-H samples are generally similar to those of the corresponding unheated samples (FIG. 5), both the Q^1 and Q^2 peaks are present. However, there are significant intensity changes with temperature. As temperature increases from 25 to 200°C, the relative intensity of the Q^2 peak increases and that of the Q^1 decreases. The FWHH of both the Q^1 and Q^2 peaks increases with increasing temperature (TABLE 2), but the two peak maxima remain resolved except for SCFUMe heated at 200°C, which yields a broad peak near -82 ppm that is more than 11 ppm wide. In addition, there may be some Q^3 sites present in the heated samples. For example the ^{29}Si MAS NMR spectrum of SCFUMe heated at 200°C contain a small shoulder near -90 to -95 ppm which is assignable to Q^3 Si-sites. These results indicate that heating of C-S-H decreases the local structural order and increases the polymerization of the structure.

Heating of the C–S–H samples also results in weight loss (TABLE 2), which can be attributed to the loss of water molecules and OH^- groups.

Thermal analysis

The TGA curves of selected C–S–H samples with different C/S ratios are similar up to 200°C but are slightly different above 200°C (FIG. 6). Within the temperature range examined, C–S–H continuously loses weight with increasing temperature, consistent with its amorphous nature. Sample CSHFS3 shows a small drop near 320°C, probably due to increased loss of OH^- groups. Samples with greater C/S ratios appear to loss more weight above 200–300°C than those with smaller C/S ratios, consistent with their content of H_2O^+ (loss on ignition) [6]. The TGA curves presented here are generally similar to those published previously [8, 9, 10], except that there are no sharp drops near 485°C, at which portlandite decomposes, consistent with the XRD results that these C–S–H samples are phase–pure [6].

The TGA curves of jennite and 1.4–nm tobermorite are different than those of C–S–H and each other. The TGA curve of 1.4–nm tobermorite is similar to those of C–S–H but indicates a much smaller rate of weight loss, whereas that of jennite has

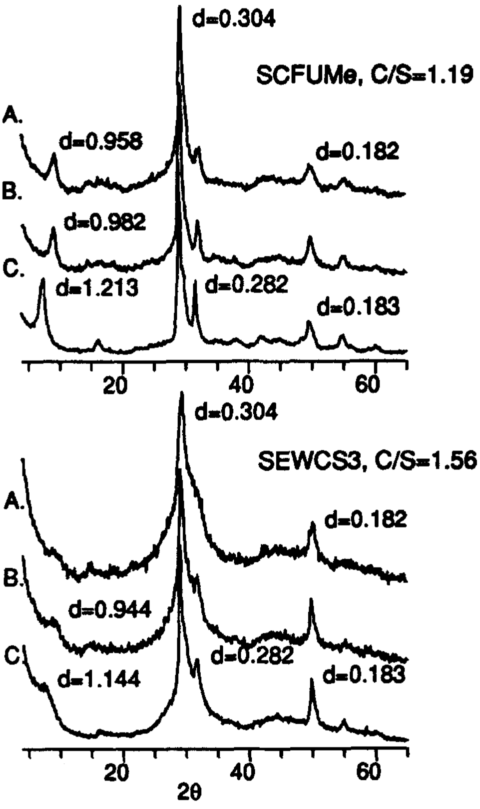

FIG. 4

XRD patterns of SCFUMe (top) and SEWCS3 (bottom) heated at different temperatures. A: 200°C; B: 110°C; and C: room temperature. The d–values are in nm.

TABLE 2

Relative Intensity (I%) and FWHH (ppm) of ^{29}Si NMR Spectra and Weight Loss (%) of C–S–H Samples Heated at Different Temperatures. The Weight Loss Is Relative to the Room Temperature (25°C) Samples. Data for SCFUMe Are Not Available due to the Broadness of the Peaks.

Sample	Temperature °C	Weight Loss (%)	Q^1		Q^2	
			I%	FWHH	I%	FWHH
SEWCS3	25		61	3.3	39	2.9
C/S=1.56	110	5.78	42	4.8	58	5.5
	200	13.17	36	4.7	64	4.9
CSHFS2	25		55	3.1	45	4.6
C/S=1.5	110	8.00	50	5.3	50	5.1
	200	12.36	48	6.0	52	5.3

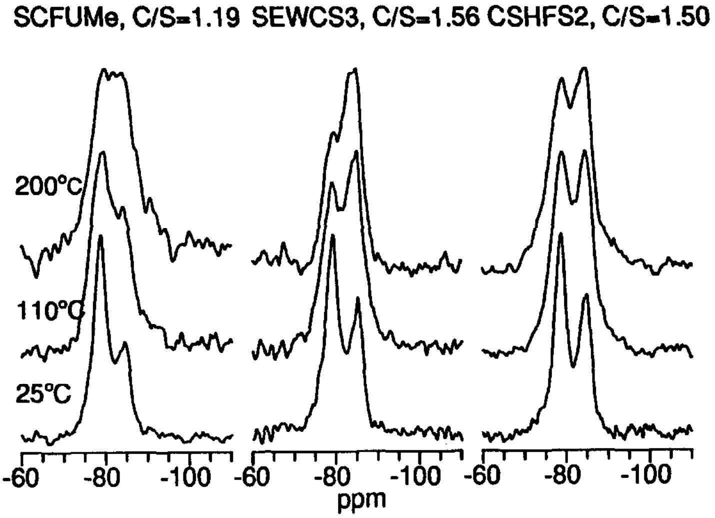

FIG. 5

^{29}Si NMR spectra of selected C–S–H heated at different temperatures as marked.

a different shape. There are two rapid drops in jennite's DTA curve. The first drop near 90°C is due to loss of water molecules and formation of metajennite and the second drop near 400°C is probably due to loss of OH$^-$ groups and formation of an ill crystalline phase [11]. These observations are consistent with the conclusion drawn by Cong and Kirkpatrick [6, 12] that C–S–H is structurally more similar to 1.4-nm tobermorite than to jennite.

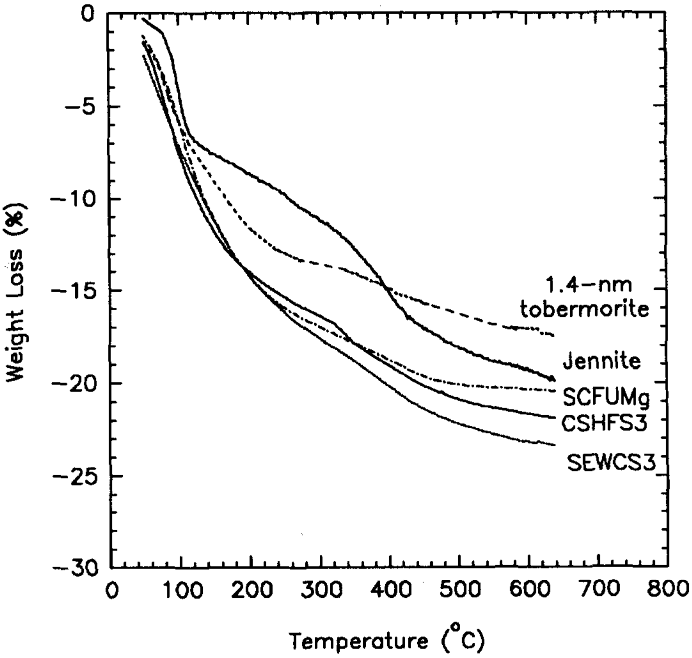

FIG. 6

Representative TGA curves for C–S–H samples SCFUMg (C/S = 0.88), CSHFS3 (C/S = 1.20) and SEWCS3 (C/S = 1.56). Also shown are the TGA curves for 1.4-nm tobermorite and jennite.

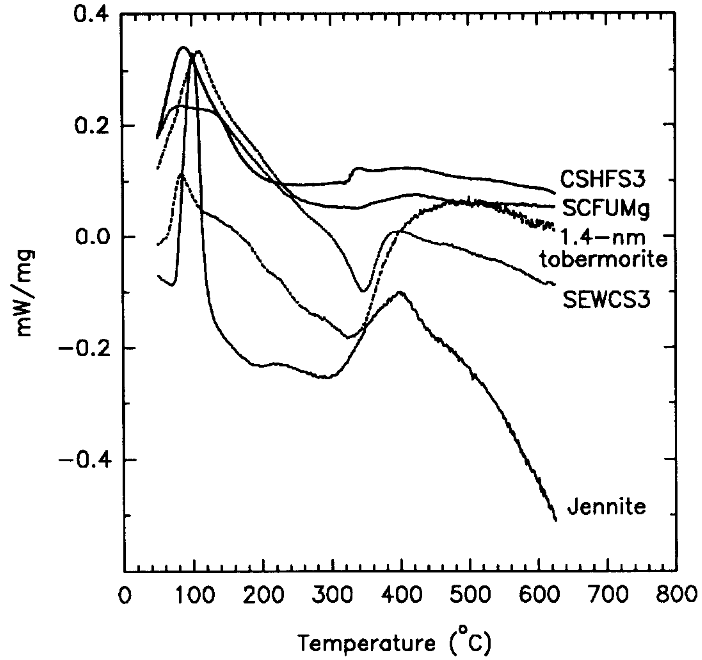

FIG. 7

Representative DSC curves for C–S–H samples SCFUMg (C/Si = 0.88), CSHFS3 (C/S = 1.20) and SEWCS3 (C/S = 1.56). Also shown are the DSC curves for 1.4–nm tobermorite and jennite.

The DSC curves of C–S–H are quite complicated and different samples behave differently (FIG. 7). All the C–S–H samples show endotherms near 100°C, which are due to loss of molecular water. As temperature increases, different C–S–H samples behave differently. There is no other major thermal event for SCFUMg (C/S=0.88). But there appears to be another small endotherm near 320°C for CSHFS3 (C/S = 1.20), consistent with the TGA data. For SEWCS3 (C/S=1.56) there is an exotherm near 350°C which is totally unexpected. XRD of this sample heated at 350°C for 1 hour in open air indicates that it decomposed and that three phases are present, residual C–S–H, vaterite (μ–$CaCO_3$) and trace of quartz. The formation of vaterite is probably due to the exposure of the sample to CO_2 in the atmosphere, which is the condition of the thermal analysis, and is thus probably the cause of the exotherm.

The DSC curve of 1.4–nm tobermorite has an endotherm near 100°C which corresponds to the loss of water molecules and formation of 1.1–nm tobermorite. There is a broad exotherm from about 100°C to 320°C, which may be related to loss of water and OH^- groups and possibly to the formation of 0.9–nm tobermorite [13]. The existence of the exotherm indicates that the formation of the 0.9–nm tobermorite may involve recrystallization, not just removal of water or OH^- groups from 1.1–nm tobermorite.

The DSC curve of jennite is quite different than those of the other phases examined. The endotherm at 90°C is due to loss of water molecules, which is responsible for the formation of meta–jennite [11]. Meta–jennite is a dehydration product of jennite by losing 7% of water and has a structure similar to that of jennite [11, 14]. The broad exotherm from about 100°C to 300°C is unexpected and cannot be attributed to formation of any known crystalline phase. Over this temperature range, meta–jennite becomes gradually dehydrated. A poorly crystalline phase forms above 375°C and the final products above 900°C are Ca_2SiO_4 and $CaSiO_3$ [11]. DSC data clearly show that jennite is structurally different than C–S–H.

Discussion

The results above indicate that the effect of decreasing relative humidity is to reduce the interlayer water content and thus decrease the basal-spacing of C–S–H, but it does not affect the polymerization of C–S–H. The effect of heating, on the other hand, is to drive out of OH^-groups as well as water molecules and thus to increase the polymerization of C–S–H and decrease its basal spacing. Both treatments of C–S–H yield a more disordered structure as shown by the broader NMR peaks.

Previous studies of the effects of relative humidity on C–S–H structure have used primarily XRD and the consensus is that decreasing relative humidity reduces the basal–spacing due to loss of interlayer water molecules [4, 5, 15]. Although we did not examine our samples with XRD due to their small size, our results support this conclusion indirectly. The CPMAS data show that the ^1H–^{29}Si coupling increases with decreasing R. H., indicating decreased proton motion and consistent with loss of water molecules. Macphee *et al.* [16] have studied the effects of relative humidity on C–S–H structure using ^{29}Si MAS NMR spectroscopy and also found that the Q^2/Q^1 ratio of most of their synthetic samples do not change with relative humidity, consistent with the present results.

The above results demonstrate that decreasing relative humidity and heating result in a more disordered structure as indicated by the greater FWHH of the ^{29}Si NMR peak for heated samples and samples cured at low R. H. Since both treatments reduce the water content of the structure, this observation thus indicates that the local Si–structural environments are different before and after the water loss. Water molecules are most likely bonded to Ca^{2+}'s in interlayer. Loss of these interlayer water results in formation of Ca–O–Si bonds and this next nearest neighbor (NNN) effect causes some changes of bond angles and distances in Si tetrahedra, and thus broader NMR peaks.

Heating of C–S–H increases polymerization, which can be expressed as

$$2Si-OH \rightarrow Si-O-Si+H_2O\uparrow .$$

Because the major change in peak intensities is decrease of Q^1 and increase of Q^2, Si–OH in above equation occurs on Q^1 sites, and Si–O–Si indicates newly formed Q^2 sites. It is clear from this equation that for every two Q^2 sites that are formed (or two Q^1 sites that are eliminated), one H_2O molecule will be lost. It is possible, therefore, to calculate the actual loss of H_2O molecules due to the polymerization change. For SEWCS3, for which the bulk composition of the original sample is known (see reference [6]), this calculation shows that only a small fraction of the weight loss (14% at 110°C and 8% at 200°C) is due to the polymerization change. Therefore, most of the lost weight must be due to water molecules, OH^- groups on Si–OH associated with Q^2 sites and OH^- groups on Ca–OH sites. Breaking down of Si–OH linkages on Q^2 sites results in formation of Q^3 sites, similar to the cross linking in 1.1–nm tobermorite [17], and may also result in formation of Si–O–Ca linkages with the interlayer Ca^{2+}'s.

The results also indicate that oven dry (110°C) of C–S–H sample is inappropriate, because at this temperature not only does the layer structure collapse, but the polymerization of silicate chains is also changed. On the other hand, drying C–S–H at reduced relative humidity (9–50%) may be adequate, because the silicate polymerization is preserved.

Conclusions

The results presented in this paper indicate that within the range of this study, heating of C–S–H has more effect on its structure than changes of relative humidity. Heating of C–S–H removes both interlayer water molecules and OH^- groups, resulting in a more polymerized and disordered structure with a smaller basal–spacing. Decreasing relative humidity appears only to remove interlayer water and thus reduce the basal–spacing, but does not change the polymerization, although the structure is more disordered.

There is more than one component of proton spin systems to the relaxation of ^{1}H–^{29}Si CP signal at higher relative humidity. At lower relative humidity, the coupling between protons and silicons becomes stronger and the CP behavior of C–S–H appears to be similar to those of the air–dried samples.

The TGA curve of C–S–H varies from sample to sample but are generally more similar to that of 1.4–nm tobermorite than that of jennite, consistent with the previous results [6]. The DSC curve of C–S–H is different for each sample and different than those of 1.4–nm tobermorite and jennite. C–S–H with the highest C/S ratio (C/S=1.56 for SEWCS3) decomposes when heated at 350°C in atmosphere, but other samples with lower C/S ratios do not.

Acknowledgments

This project was supported by the National Science Foundation Center for Science and Technology of Advanced Cement–Based Materials (ACBM).

References

[1] Young, J. F. *J. Am. Ceram. Soc.*, 71, C–118, (1988).
[2] Hirljac, J.; Wu, Z. Q.; Young, J. F. *Cem. Concr. Res.*, 13, 877, (1983).
[3] Ishida, H.; Sasaki, K.; Okada, Y.; Mitsuda, T. *J. Am. Ceram. Soc.*, 75, 2541, (1992).
[4] Smith, R. H.; Bayliss, P. *Cem. Concr. Res.*, 2, 643, (1972).
[5] Gutteridge, W. A.; Parrott, L. J. *Cem. Concr. Res.*, 6, 357, (1976).
[6] Cong, X.; Kirkpatrick, R. J. *submitted to Advn. Cem. Bas. Mat.*
[7] Cong, X.; Kirkpatrick, R. J. *Adv. Cem. Res.*, (in press).
[8] Greenberg, S. *J. Phys. Chem.*, 58, 362, (1954).
[9] Taylor, H. F. W.; Turner, A. B. *Cem. Concr. Res.*, 17, 613, (1987).
[10] James, J.; Rao, M. S. *Cem. Concr. Res.*, 16, 67, (1986).
[11] Carpenter, A. B.; Chalmers, R. A.; Gard, J. A.; Speakman, K.; Taylor, H. F. W. *Am. Mineral.*, 51, 56, (1966).
[12] Cong, X.; Kirkpatrick, R. J. *submitted to J. Am. Ceram. Soc.*
[13] Farmer, V. C.; Jeevaratnam, J.; Speakman, K.; Taylor, H. F. W. Thermal decomposition of 14 Å tobermorite from Crestmore. in *Symposium on Structure of Portland Cement Paste and Concrete (Sp. Rpt. 90)*, pp 291–98, Washington, Highway Research Board, (1966).
[14] Gard, J. A.; Taylor, H. F. W.; Cliff, G.; Lorimer, G. W. *Am. Mineral.*, 62, 365, (1977).
[15] Smith, R. H.; Bayliss, P.; Gamble, B. R.; Mills, R. H. *Cem. Concr. Res.*, 2, 559, (1972).
[16] Macphee, D. E.; Lachowski, E. E.; Glasser, F. P. *Adv. Cem. Res.*, 1, 131, (1988).
[17] Cong, X.; Kirkpatrick, R. J. *submitted to Advn. Cem. Bas. Mat.*